JANUARY 06 2026

Nearfield directivity analysis during the NG-19 launch

Micah R. Shepherd ; Carson F. Cunningham; Kent L. Gee

Proc. Mtgs. Acoust. 56, 040006 (2025)
https://doi.org/10.1121/2.0002207

Volume 56 http://acousticalsociety.org/

ASA/ICA 2025 New Orleans

188th Meeting of the Acoustical Society of America
joint with
25th International Congress on Acoustics

New Orleans, Louisiana
18-23 May 2025

Noise: Paper 4pNS8

Nearfield directivity analysis during the NG-19 launch

Micah R. Shepherd, Carson F. Cunningham and Kent L. Gee
Department of Physics and Astronomy, Brigham Young University, Provo, UT, 84602, USA; shep@physics.byu.edu; kentgee@byu.edu; carsonfc@byu.edu

In August 2023, the Antares 230 launched successfully for the NG-19 resupply mission to the International Space Station. Acoustic measurements were taken at various locations around the launch pad, ranging from 60 to 200 m away from the vehicle. The analysis focused on azimuthal and polar angles to investigate the vehicle's sound directivity during the launch. Spectral data were evaluated as functions of frequency, angular position around the pad, and orientation relative to the vehicle. A spatio-spectral analysis was conducted to interpret the data effectively. Initial findings reveal that maximum sound levels are associated with wider angles relative to the plume for stations closer to the source. The peak frequency at all stations was observed to be between 20 and 60 Hz, which is common for vehicles of this size. Although proximity to the rocket complicates distinguishing between angles, making directivity analysis challenging, a spatio-spectral analysis best reveals the spectral features of the noise.

Proceedings of Meetings on Acoustics, Vol. 56, 040006 (2025); https://doi.org/10.1121/2.0002207.

1. INTRODUCTION

This paper will discuss several aspects of rocket acoustics observed in the acoustic data collected during the Antares 230+ launch in August 2023. More specifically, this paper will show how traditional interpretations of the sound power spectrum, peak directivity angle, and source region are impacted when measurements are made near the launch pad and flame trench. To begin, each of these quantities will be briefly discussed.

Total sound power is an important metric for acoustic characterization and comparison between launch vehicles. It does not inherently depend on distance but is most easily computed when measurements are made far away from the source to ensure that the sound flux is entirely outward. A deeper look into sound power comes from calculating the sound power spectrum when the sound power spectrum is divided into individual power values for each frequency. Again, it is a useful tool for comparison between launch vehicles, especially when normalized and plotted against Strouhal number. The common normalization factor is D_e/U_eW_{max}, where D_e is the nozzle diameter, U_e is the exit velocity and W_{max} is the maximum sound power.[1]

Another key aspect of launch acoustics is rocket noise directivity, which describes the directional distribution of sound energy emitted during operation. Understanding the directional properties of rocket noise is crucial for predicting the areas experiencing the most intense acoustic loads and developing protective measures for payloads and ground support equipment. Polar directivity describes the angle at which the peak acoustic radiation occurs relative to the exhaust plume. Previous rocket acoustics studies have demonstrated that the polar angle giving the peak level is typically observed at an angle near 70° from the exhaust plume, a phenomenon attributed to Mach wave radiation.[2–4] A method for quantifying this behavior uses the convective Mach number, which incorporates the exhaust velocity—dependent on nozzle dimensions—to predict the jet's directional radiation lobe.[5] Experimental validation of this method has been achieved through controlled studies involving both jet engines and rocket systems. However, jet-based experiments have typically been conducted under idealized conditions, where the jet remains stationary, and the surrounding environment is free of elements that could introduce distortions, scattering, or reflections. Rocket acoustics studies rarely have this luxury and instead will often make measurements away from buildings and other structures to avoid the effect of reflections and scattering. Thus, the effect that being near the pad has on the peak directivity angle is not entirely known. Naturally, near field effects may also impact measurements when equipment is in the vicinity of the plume.

A third concept that is important for understanding rocket acoustics is the location and amplitude of the acoustic source within the plume. Though some discrepancies exist in the older literature,[6] the dominant location of the source is within the supersonic region. The generally accepted source position range is defined in terms of effective nozzle diameters and ranges from 6-30 D_e downstream, depending on frequency.[7] For acoustic models far away from the plume, a compact region located at $18D_e$ has been used with good accuracy.[2] This range of accepted values assumes an undeflected, fully-formed plume. The source location for a fully or partially deflected plume has not been exhaustively studied.

To collect the data used for this analysis, five measurement stations were placed at various distances and angles around the pad, as shown in Fig. 1 and listed in Table 1. The stations used GRAS 46BG or 46BD 1/4" microphones placed 1/4" above a circular ground plate. The microphones were oriented downward close to the ground to minimize the effect of ground reflections and then covered with a windscreen to minimize the influence of wind noise. Measurements were

taken at a sample rate of 102.4 kHz over the duration of the launch. This measurement configuration has been successfully used in other rocket acoustics studies and is described in more detail by Cunningham et al[8] or Anderson.[9]

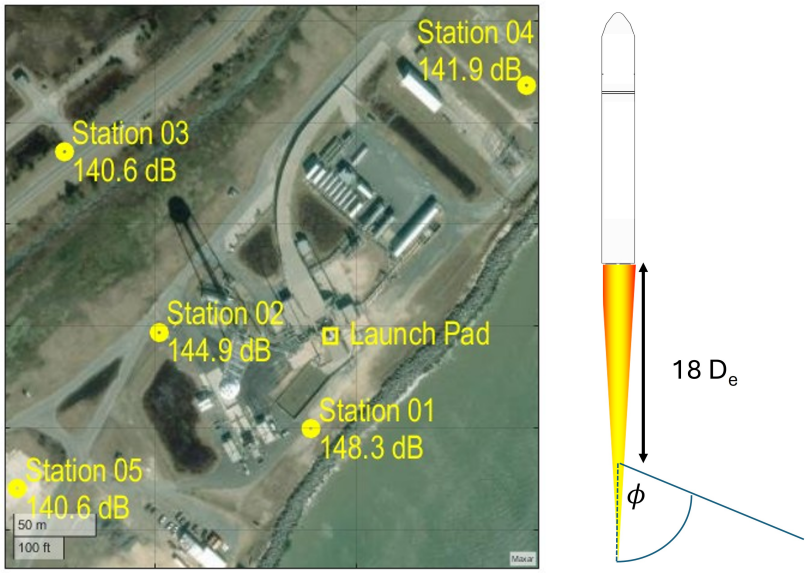

Figure 1: (left) Aerial map of the station locations surrounding the launch pad, along with maximum measured levels. (right) Illustration of the polar angle that begins after 18 ***effective nozzle diameters*** (D_e) ***emerges from the flame trench.***

Table 1: Maximum overall sound pressure level $(OASPL_{max})$ ***for each station along with the approximate orientation and distance to the vehicle.***

Station	Orientation	Distance (m)	$\mathbf{OASPL_{max}}$
1	S	60	148.3 dB
2	W	100	144.9 dB
3	NW	192	140.6 dB
4	NE	193	141.9 dB
5	SW	209	140.6 dB

2. SOUND POWER SPECTRUM

Sound power calculations were made from each of the five stations to assess consistency across location. The procedure used to calculate the sound power, as outlined in Kellison and Gee,[10] should yield the same overall sound power for each station, assuming all of the assumptions of the method are met. The results indicate an average sound power level of 191.5 dB ± 0.8 dB across the five measurement stations. The acoustic efficiency of the rocket is then estimated to be between 0.37% - 0.53%. This is a wider range of acoustic efficiency values than is typically reported and is directly due to the variability in the levels measured at each station.

The variation is explored further by calculating the sound power spectrum. Fig. 2 (left) shows the sound power spectra with reasonable similarity between each station. The stations all have a peak frequency near 30 Hz, with slightly varying amplitudes. Station 4 clearly shows a small boast in peak magnitude compared to the other stations. Since sound power should not depend on distance away from the source, nor its location relative to the rocket, these differences suggest that some of the underlying assumptions for sound power calculation might not hold. However, when the sound power spectrum is non-dimensionalized, as shown in Fig. 2 (right), all 5 stations collapse very well over the majority of Strouhal numbers. The largest variations are seen at Strouhal numbers below 0.006. This indicates that each station is a sufficient distance from the vehicle for the assumptions of sound power to be reasonably valid, except at very low frequencies. The sound power spectrum model given by Eldred in the NASA report SP-8072 is also plotted in Fig. 2 (right).[1] The peak Strouhal number of the model (St=0.018) matches well with the measured data but is at a lower normalized level. Also, the measured spectra decrease with frequency at a faster rate than the model.

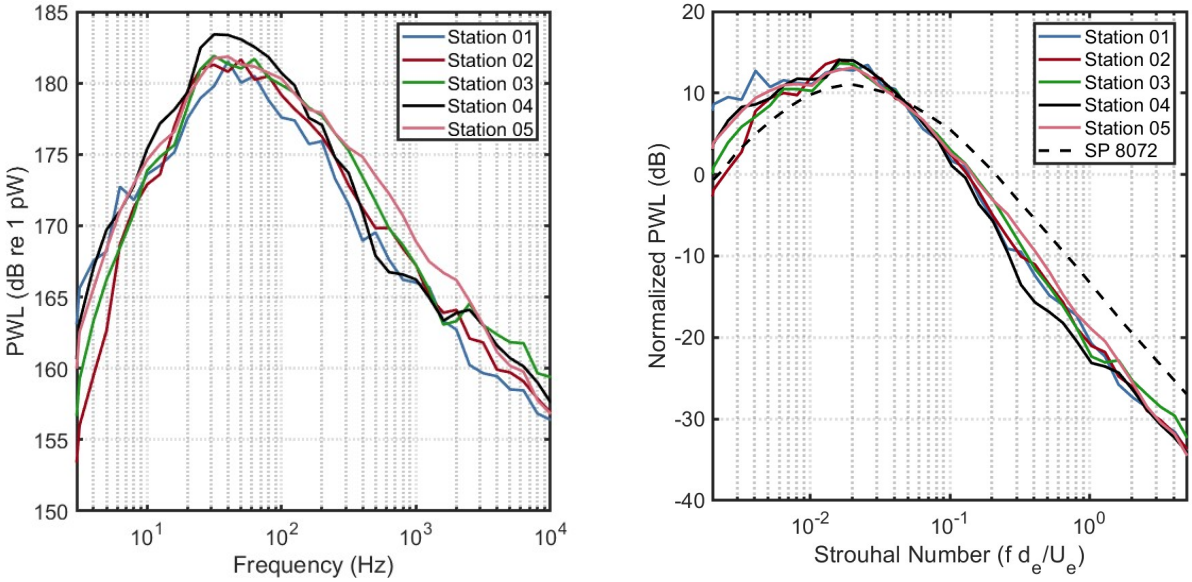

Figure 2: (left) Sound power level (PWL) spectra as a function of frequency for all five stations. (right) Normalized PWL spectra ($W/W_{max} \cdot U_e/D_e$) as a function of Strouhal number (fD_e/U_e).

3. DIRECTIVITY RESULTS

For directivity calculations, it is important to note that a far-field point source assumption is typically used. For these calculations, the source location is set $18D_e$ downstream of the nozzles. Since the stations are not necessarily in the far-field, the distributed nature of the source may be evident.[11–13] This is acknowledged, but the computations will still be useful as a comparison, and to see how this point source impacts directivity calculations. As the source is deflected and remains inside the flame trench for the first few seconds during launch, the directivity calculations will not

begin until after the acoustic point source has reached the level of the deck, as shown in Fig. 1. The station positions and maximum OASPL are also shown in Fig. 1 for reference.

A. DETERMINATION OF PEAK ANGLE

As an introduction to our noise analysis, Fig. 3 (left) shows how the max levels at each station differ and at what times relative to liftoff the highest levels occur. When the effect of distance is removed from each station by normalizing to a common distance (chosen arbitrarily to be 100 D_e), important distinctions between stations can be seen (see Fig. 3 (right)). First, the spectra do not collapse to a common shape or level. Station 1 is the biggest outlier, having a max level several dB lower than stations 3 - 5. This indicates that the noise does not obey the same spreading laws at all the stations despite the sound power spectra being similar. This is likely caused by station 1 being close enough to the deflected plume that significant extended source effects are present. This could also be an indication of a directional lobe or some other form of asymmetry in the acoustic data. However, the results in Fig. 3 (right) are not enough to be conclusive and additional analysis are necessary.

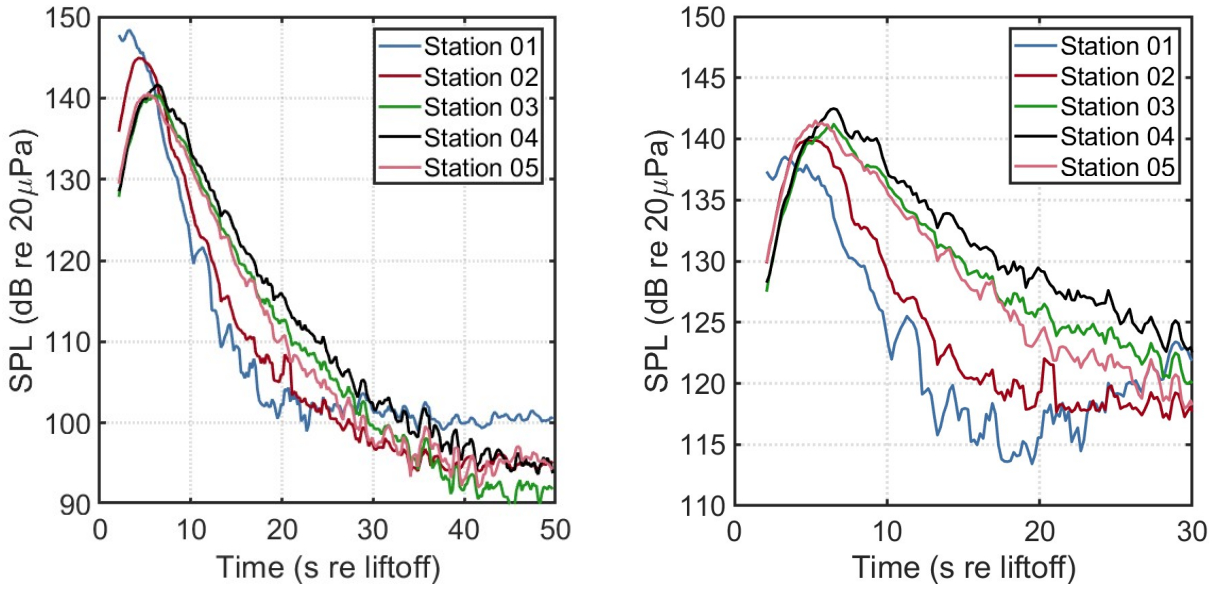

Figure 3: (left) Sound pressure levels as a function of time referenced to liftoff. The distance from the center of the launch pad to each station is shown in Table 1. (right) Distance-normalized sound pressure levels as a function of time reference to liftoff.

The peak directivity angle was found to be around 70° relative to the plume using trajectory data. This is in-line with measurements from similar rockets.[14] To examine this more closely, the OASPL from Fig. 3 were plotted against the altitude angle, the angle from each station to the 18 D_e downstream on the rocket nozzle, and normalized by distance (see Fig. 4). The data in the figure starts near 90°, indicative of the rocket resting on the pad prior to liftoff. As the rocket increases in altitude, the angle decreases and the angle where the SPL is highest indicates the peak directivity angle. It is apparent in Fig. 4 that the peak angles do not match for each station. Station 5 shows a peak angle near 70°, whereas stations 2, 3 and 4 have a peak angle of roughly 60°. The SPL values

for station 1 are not characteristic of rocket noise at all, with the levels from 85° to 35° all being within 3 dB. Also of note is that station 2 has an uncharacteristically wide angular peak, centered around 60° but stretching ±10°. The fact that the peak levels are being sustained over a wide range of altitude angles may be simply due the non-compact nature of the source. However, since the sound power estimates seemed to collapse, it could also be a result of pad or trench effects. Clearly, the expected $\theta_{pk} = 70°$ is not lining up with the data in the initial time after ignition.

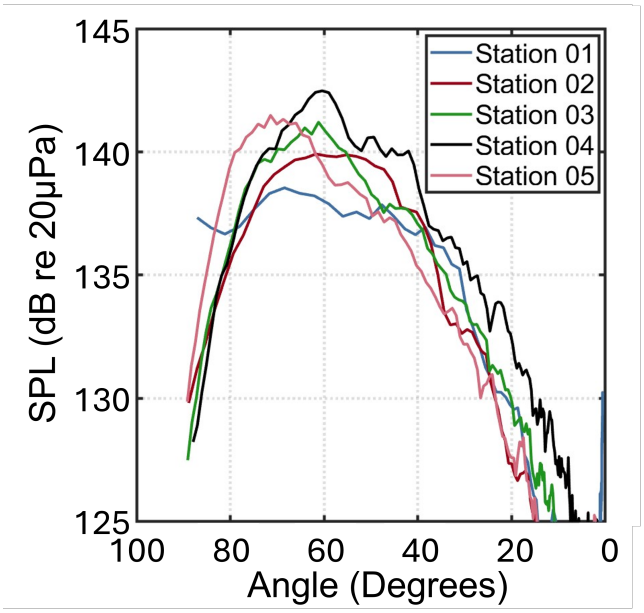

Figure 4: Overall sound pressure level at various angles relative to the rocket plume for each station.

B. SPATIO-SPECTRAL ANALYSIS

A different way to investigate this behavior is through spatio-spectral analysis. Spatio-spectral methods have been successfully applied to characterize the near-field directivity of jet noise under controlled conditions. The technique is similar to time-frequency spectrograms but uses space instead of time (using the relationship between time, vehicle location and plume angle) to determine the spatial and spectral properties of the noise field. In this manner, directional trends in the acoustic data can be examined.[15–17] Given their effectiveness in jet noise studies, spatio-spectral methods will be used to investigate this data set for evidence of launch pad and trench effects.

Figure 5 displays the spatio-spectral plots for three stations, with contour lines indicating a 3 dB reduction in levels. The deepest red portions of the figure indicate the frequency and angle at which the noise level is highest for that station. At Station 1, a band of high sound levels ranging from 25 to 60 Hz are evident between 40° and 70°. The maximum value occurs around 40 Hz as the vehicle reaches 50°. Again, this does not follow the commonly-accepted characteristics of rocket noise. Station 4 records its highest amplitude in the region between 25 and 40 Hz and for angles ranging from 57° and 63°. A small noise hot spot also occurs at 40 Hz and 50°. As a note, stations 2 and 3 are not shown due to their similarity to stations 1 and 4, respectively. The spatio-

spectrogram for station 5 is similar to station 4 but has levels shifted to higher angles and higher frequencies. A distinct maximum level occurs at 50 Hz and 67°.

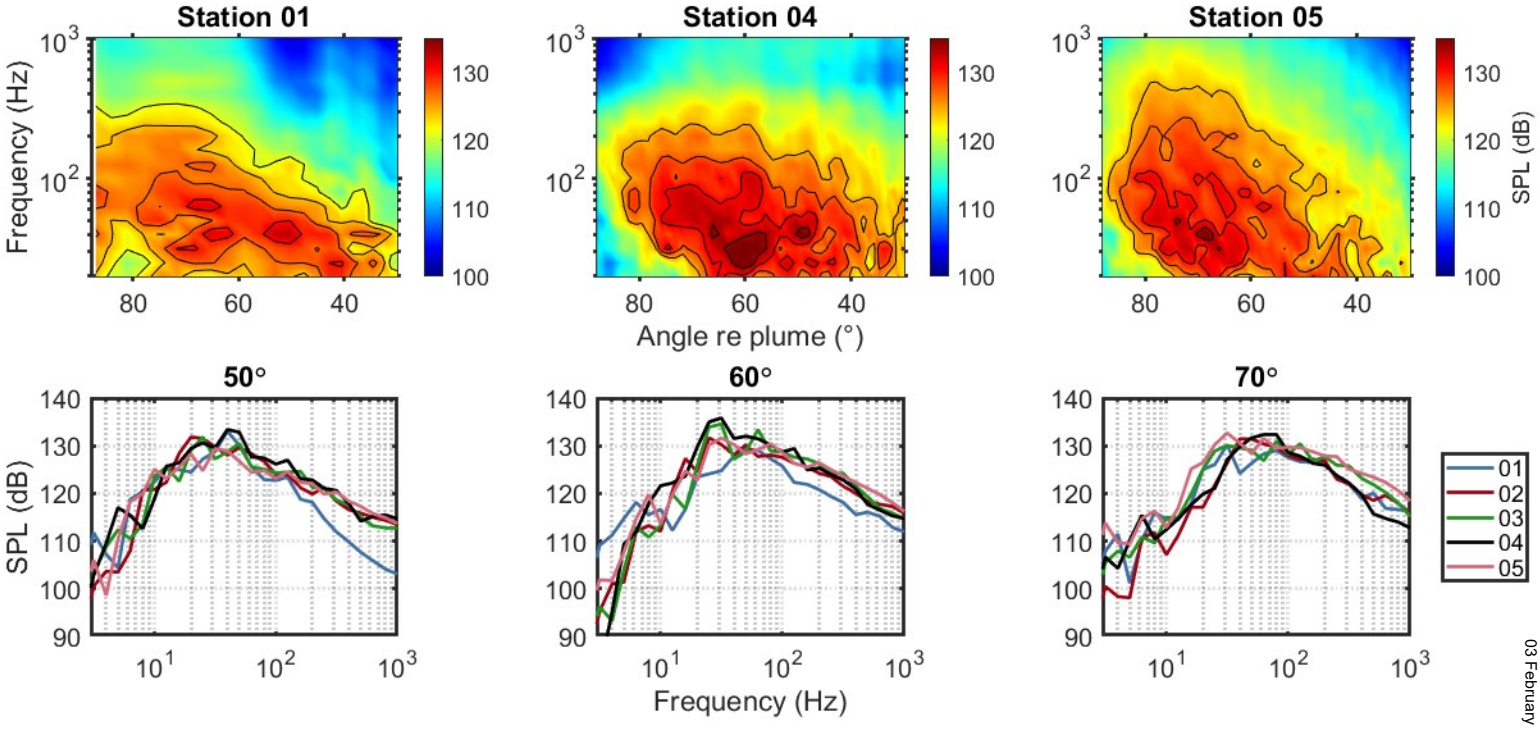

Figure 5: (Top) Spatio-spectral plots for three stations where the contour lines define decreasing 3 dB increments from the maximum level, and (bottom) spectra slices at 50, 60, and 70°.

Since the expected peak directivity angle is 70° , it is significant that several of the stations show the highest peak to be at 60°. By looking at the 60° slice of the spatio-spectra, it is easier to determine the frequency content at that angle (bottom-middle of Fig. 5). The 50°and 70°slices are also shown as a reference. These slices show that station 1 can have a difference up to 8 dB compared to the other stations for certain frequencies and angles. This suggests that there might be directivity differences or pad effects that are happening more severely at station 1 than the other stations. The plume impinging on the deck could also play a bigger role at station 1 due to its proximity to the trench.

Another explanation for why the peak directivity angles differ from each other is that the assumed source location (i.e. $18D_e$) is incorrect during these early times. Due to the proximity to the vehicle, a point source assumption is certainly not completely valid. Instead, the source would be seen at the stations as an extended region rather than a point. Additionally, relatively small changes in the source position could account for the differences, such that using 18 D_e inherently biases the results. The inconsistent behavior between stations could also come from different pad or trench effects where one or more of the station have unique contributions to the sound from reflections, scattering or other disturbances of the surrounding structures. This seems particularly true for station 1.

4. EXPLORATION OF SOURCE REGION

While earlier sections presented measured directivity angles and spatio-spectral characteristics, they were limited by the assumption of a source position within the plume. This section assumes instead that the Mach wave radiation angle is maintained during liftoff. Specifically, the peak directivity angle is assumed to stationary such that it can be estimated using formulations based on rocket flow parameters, namely the jet velocity. A basic model for the convective Mach number will be used, which has been shown to be accurate for estimating the peak directivity angle of several supersonic jets and rockets.[5] These comparisons help evaluate whether observed angular trends are consistent with established far-field theory or indicate more complex near-field behavior.

A simple definition of convective Mach number (M_c) will be used:

$$M_c = \frac{U_c}{c}, \tag{1}$$

where c is the ambient sound speed and U_c is the convective velocity of the jet. U_c is often estimated to be 70% of the centerline velocity of the jet. The peak directivity angle is then found using

$$\theta_{pk} = \cos^{-1}\left(\frac{1}{M_c}\right). \tag{2}$$

It has recently been shown that $M_c \approx \sqrt{M}$, where M is the jet acoustic Mach number.[5] Thus, with only knowledge of the jet velocity and the ambient sound speed, θ_{pk} can be estimated. Using this simple formula and a sound speed $c = 340$ m/s, we obtain a peak directivity angle of 70.6°. Although the ambient speed of sound varies with altitude and temperature, the overall effects of these deviations on θ_{pk} are relatively small.

As a note, a more advanced form of the convective Mach number could be used, such as the so-called Oertel convective Mach number:

$$M_c = \frac{U_j + 0.5c_j}{c_j + c}. \tag{3}$$

Here, c_j is the speed of sound within the plume and U_j is the fully expanded jet velocity (see Ref. [5] for details). Using this form of M_c yields a predicted angle of $69.7°$, less than $1°$ different than when using the simpler form of M_c. However, the value to use for c_j is not straightforward to estimate with high accuracy. Thus, using the Oertel convective Mach number to estimate θ_{pk} adds additional uncertainty and therefore isn't necessarily more accurate than using the simple definition of M_c.

While these formulations are generally intended for predictions beyond approximately $250D_e$ downstream,[18,19] the farthest recording station (station 5) is 218 D_e and produces a measured peak angle of approximately $70°$ using farfield integration. By assuming the Mach wave radiation does not change during liftoff, we can estimate some aspects of the extended nature of the source. Essentially, this portrays an "apparent" or "effective" source region as a function of frequency which is created by the complex effects of the pad and flame trench. When the effective source region differs for each station, this indicates that the pad and trench effects depend on location. Based on the previous analysis, this is the expected behavior. When the effective source region from each station collapses, there are two possibilities: 1) the pad and trench effects are negligible or 2) the pad or trench effects are the same for each station.

Figure 6 shows the distance normalized SPL as a function of normalized height rather than angle. This shows exactly how far the vehicle has risen during the max levels and can be used to determine the effective source region by determining the height of the rocket during which the SPL is within 1 dB of the maximum level. Table 2 shows the estimates of the effective source region for each station. The results for Station 1 are quite different than the other stations, likely due to its proximity to the trench. Since the deflected plume acts like a second nozzle oriented 90°from the rocket, it strongly influences the noise and creates acoustical characteristics that are not traditionally seen in rocket noise. Stations 2 - 5 appear to have more traditional values, though station 2 differs somewhat from 3 - 5. Thus, the pad and trench effects at station 2 are different than stations 3 - 5 possibly due to it being nearly 100m closer to the pad than 3 - 5. Interestingly, stations 3 - 5 show similar source regions even though they are on opposite sides of the pad. This suggests that when far enough away, the effects of the pad and trench blend together such that their overall effect does not strongly depend on the position of the station.

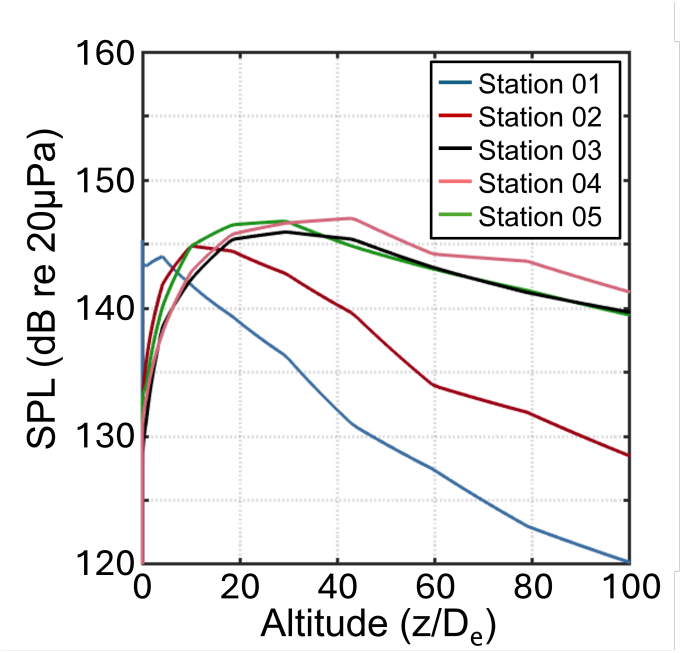

Figure 6: The maximum SPL for a single microphone from each station as a function of normalized altitude of the rocket. The level is distance normalized to 100 D_e.

Table 2: "Effective" extended source region given in jet diameters downstream of the nozzle. A constant peak directivity angle is assumed and the amplitude is normalized by distance.

	Station 1	**Station 2**	**Station 3**	**Station 4**	**Station 5**
Source Begins (D_e)	0	7	17	16	15
Source Ends (D_e)	6	22	50	50	35

The results from this section suggest that early-time rocket noise (i.e. within approximately 15 s of liftoff) cannot be adequately described near the pad using a fixed point source model. While

being near the pad does not effect the sound power spectrum, it does impact the maximum sound pressure level as shown using spatio-spectral analysis. Additionally, assuming a fixed point source leads to a peak directivity angle that depends on microphone position and cannot be accurately predicted with standard methods. There are a number of factors which could cause the point source model to fail including nearfield effects, plume impingement effects and launch structure effects (including the flame trench).

By assuming consistent undeflected behavior of the plume, Mach wave radiation could be estimated using a simple prescribed theory. With this assumption, the aggregate effect of all of the complicated early-time factors can be lumped together into an effective source region which depends on the position of the station. It is possible that the effective source region could then be used for early-time modeling of the noise, though additional work would be necessary to validate this approach.

5. CONCLUSION

This paper summarizes the acoustic results from the Antares 230+ NG-19 launch in August 2023. The acoustic stations were placed between 60 - 209 m from the pad such that pad and flame trench effects were evident. The sound power spectrum collasped for all of the stations but the peak directivity angle and extended source region are shown to dependent on location. Thus, a fixed-point model cannot be used to accurately describe the noise in the initial seconds after liftoff. Spatio-spectral analysis was used to identify directional sound radiation inconsistencies between stations. An apparent sound region was then presented to account for all of the effects which influence the sound field right after launch. These results underscore the need to treat near-field directivity as distinct from far-field approximations.

To conclude, we assert that common metrics used to describe far field rocket noise measurements should not be used to on rocket noise data collected near the pad without careful scrutiny. Future work should aim to refine nearfield models of rocket noise, leveraging spatio-spectral methods and trajectory-based localization to improve predictions of launch-induced acoustic environments during the early stages of the launch.

ACKNOWLEDGMENTS

The authors acknowledge the Northrup Grumman Corporation for funding this work. The authors also thank Peter Jensen, Jacob Sampson, Makayle Kellison and Zach Hendry for assisting with data collection.

REFERENCES

[1] Kenneth M. Eldred. Acoustic loads generated by the propulsion system. Technical report, NASA SP-8072, 1971.

[2] Caroline P. Lubert, Kent L. Gee, and Seiji Tsutsumi. Supersonic jet noise from launch vehicles: 50 years since NASA SP-8072. *The Journal of the Acoustical Society of America*, 151(2):752–791, 02 2022.

[3] Max Kandula. Near-field acoustics of clustered rocket engines. *Journal of Sound and Vibration*, 309(3):852–857, 2008.

[4] Ch L Xing, G G Le, Ch F Zhao, and H Zheng. Investigations on the influence of one and two-sided jet deflector on acoustic environment of multi-nozzle launch vehicle at lift-off. *Journal of Physics: Conference Series*, 1507:102015, 2020.

[5] Kent L. Gee, Tyce W. Olaveson, and Logan T. Mathews. Convective mach number and full-scale supersonic jet noise directivity. *AIAA Journal*, 0(0):1–12, 2024.

[6] Kent L. Gee. A tale of two curves and their influence on rocket and supersonic jet noise research. *The Journal of the Acoustical Society of America*, 149(4):2159–2162, 04 2021.

[7] Kent L. Gee, Eric B. Whiting, Tracianne B. Neilsen, Michael M. James, and Alexandria R. Salton. Development of a near-field intensity measurement capability for static rocket firings. *Transactions of the Japan Society for Aeronautical and Space Sciences, Aerospace Technology Japan*, 14(ists30):Po–2–9 – Po–2–15, 2016.

[8] Carson F. Cunningham, Mark C. Anderson, Levi T. Moats, Kent L. Gee, Grant W. Hart, and Lucas K. Hall. Acoustical measurement and analysis of an atlas V launch. *Proceedings of Meetings on Acoustics*, 46(1):045005, 06 2023.

[9] Mark C. Anderson. Weather-robust systems for outdoor acoustical measurements. *Brigham Young University Senior Thesis (https://physics. byu. edu/department/theses/gee/2021)*, 2021.

[10] Makayle S. Kellison and Kent L. Gee. Sound power of NASA's lunar rockets: Space Launch System versus Saturn V. *JASA Express Letters*, 3(11):113601, 11 2023.

[11] Robert C. Potter and Malcolm J. Crocker. Acoustic prediction methods for rocket engines, including the effects of clustered engines and deflected exhaust flow. NASA Contractor Report NASA-CR-566, NASA, Washington, DC, 1966.

[12] William H. Mayes, Wade E. Lanford, and Harvey H. Hubbard. Near-field and far-field noise surveys of solid-fuel rocket engines for a range of nozzle exit pressures. NASA Technical Note D-21, NASA, Washington, DC, 1959.

[13] Kent L. Gee, Robert J. Kenny, Tracianne B. Neilsen, Trevor W. Jerome, Chrisopher M. Hobbs, and Michael M. James. Spectral and statistical analysis of noise from reusable solid rocket motors. In *Proceedings of Meetings on Acoustics*, volume 18, page 040002, 2013.

[14] Grant W. Hart, Kent L. Gee, and Mylan R. Cook. Corrected frequency-dependent directivity indices for large solid rocket motors. *Proceedings of Meetings on Acoustics*, 51(1):040007, 12 2023.

[15] Logan T. Mathews and Kent L. Gee. Acoustical holography and coherence-based noise source characterization of an installed f404 engine. *AIAA Journal*, 62(6):2186–2199, 2024.

[16] Kevin M. Leete, Alan T. Wall, Kent L. Gee, Tracianne B. Neilsen, Michael M. James, and J. Micah Downing. Acoustical holography-based analysis of spatiospectral lobes in high-performance aircraft jet noise. *AIAA Journal*, 59(10):4166–4178, 2021.

[17] Tyce W. Olaveson, Jacob Ward, Jon P. Johnson, Kent L. Gee, and Alan T. Wall. Analysis of spatiospectral lobes in installed F404 engine noise radiation. *28th AIAA/CEAS Aeroacoustics 2022 Conference*, 2022.

[18] Michael M. James, Alexandra R. Salton, Kent L. Gee, Tracianne B. Nielsen, Sally A. McInerny, and Robert J. Kenny. Modification of directivity curves for a rocket noise model. *Proceedings of Meetings on Acoustics*, 18:040008, 2014.

[19] Sally A. McInerny. Launch vehicle acoustics part 1: Overall levels and spectral characteristics. *J. Aircraft*, 33(3):51–517, 1996.